catalysts

MDPI

Article

New Approach to Synthesis of Tetralin via Naphthalene Hydrogenation in Supercritical Conditions Using Polymer-Stabilized Pt Nanoparticles

Alexey V. Bykov [1], Daria V. Alekseeva [1], Galina N. Demidenko [1], Alexandre L. Vasiliev [2], Linda Nikoshvili [1,3,*] and Lioubov Kiwi-Minsker [3,4,*]

1 Department of Biotechnology, Chemistry and Standardization, Tver State Technical University, A.Nikitina Street, 22, 170026 Tver, Russia; bykovav@yandex.ru (A.V.B.); dashka2433@gmail.com (D.V.A.); xt345@mail.ru (G.N.D.)
2 National Research Centre, Kurchatov Institute, 123182 Moscow, Russia; a.vasiliev56@gmail.com
3 Regional Technological Centre, Tver State University, Zhelyabova Street, 33, 170100 Tver, Russia
4 Ecole Polytechnique Fédérale de Lausanne, GGRC-ISIC-EPFL, CH-1015 Lausanne, Switzlerand
* Correspondence: nlinda@science.tver.ru (L.N.); lioubov.kiwi-minsker@epfl.ch (L.K.-M.); Tel.: +7-904-005-7791 (L.N.); +41-21-693-3182 (L.K.-M.)

Received: 3 November 2020; Accepted: 20 November 2020; Published: 23 November 2020

Abstract: Supercritical (SC) fluid technologies are well-established methods in modern green chemical synthesis. Using SC fluids as solvents instead of traditional liquids gives benefits of higher diffusivity and lower viscosity, which allows mass transfer intensification and, thus, an increased production rate of chemical transformations. Therefore, a conjugation of heterogeneous catalysis with SC media is a large step toward a green chemistry. Tetralin (TL) is an important hydrogen donor solvent used for biomass liquefaction. In industry, TL is obtained via catalytic hydrogenation of naphthalene (NL). Herein, for the first time we have demonstrated the NL hydrogenation with close to 100% selectivity to TL at almost full conversion in the SC hexane. The observed transformation rates in SC hexane were much higher allowing process intensification. The downstream processes can be also facilitated since hexane after depressurisation can be easily separated from the reaction products via simple rectification. The TL synthesis was studied in a batch reactor at variation of reaction temperature and overall pressure. For the first time for this process, low Pt-loaded (1 wt.%) nanoparticles stabilized within hyper-cross-linked aromatic polymer (HAP) were applied. The Pt/HAP catalyst was stable under reaction conditions (250 °C, 6 MPa) allowing its recovery and reuse.

Keywords: tetralin; naphthalene; supercritical hexane; hydrogenation; platinum nanoparticles; hyper-cross-linked aromatic polymer

1. Introduction

Heterogeneous catalytic processes are considered as sustainable due to the possibility of catalyst recovery and recycling [1,2]. Supercritical (SC) fluid technologies are well-established in modern green chemical synthesis [3]. Using SC fluids as solvents instead of traditional liquids gives the benefits of higher diffusivity and lower viscosity, which allows mass transfer intensification and, thus, an increased production rate of chemical transformations [4]. Therefore, a conjugation of heterogeneous catalysis with SC media is a large step toward a green chemistry.

The environmental impact of global warming, caused by greenhouse gases, promoted the use of biomass, as it creates less environmental pollution and diminish health risks than fossil

fuel combustion. Liquefaction of biomass using hydrogen donor (HD) solvents is a promising route to obtain clean high-quality biofuel. Tetralin (TL) is an important HD solvent for biomass liquefaction, which simultaneously serves as a stabilizing medium, a heat carrier and a trap for the formed radicals preventing their recombination.When deprived of two hydrogen atoms, TL enters the rearrangement resulting in naphthalene (NL) production. This process requires the regeneration of TL via hydrogenation of NL [5–9].

In industry TL is obtained via selective catalytic hydrogenation of naphthalene (NL) and generally follows the reaction scheme shown in Figure 1. According to this scheme, two moles of hydrogen spent per one mole of naphthalene lead to the formation of TL. Under certain reaction conditions in the presence of a catalyst, TL can be further hydrogenated to *cis*-DL and *trans*-DL while accepting three moles of hydrogen molecules per one mole of TL. Another way of TL transformation, as well as of the formed DLs, is hydrogenolysis or cracking with the opening of saturated cycles. It is noteworthy that the reaction of TL hydrogenation to DLs usually prevails over TL degradation reactions [5,10,11].

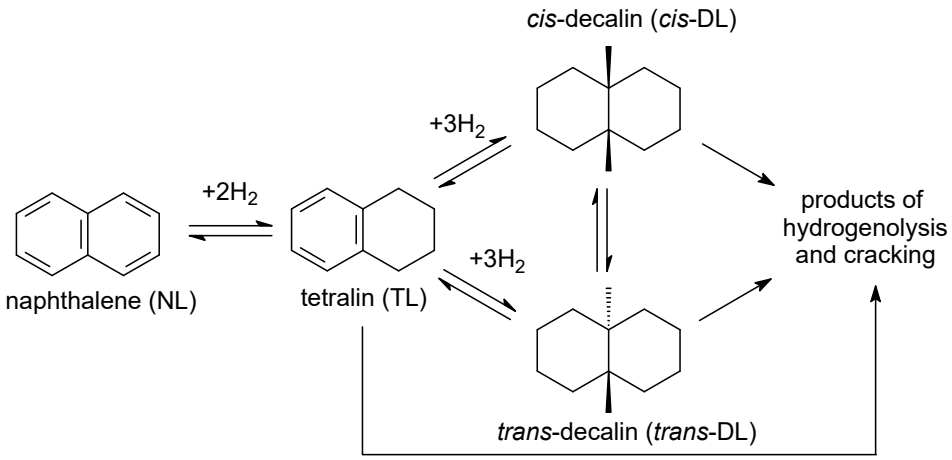

Figure 1. Schematic presentation of naphthalene (NL) hydrogenation.

Hydrogenation of NL is well studied in gas-phase and liquid-phase processes [5,6,9,12–14]. A few studies have reported data on the hydrogenation of aromatics in SC CO_2 [15,16] but, to date, there are no reports on TL catalytic synthesis in SC solvent (i.e., hexane) conditions. The best catalytic systems of NL hydrogenation are based on nanoparticles (NPs) of platinum, palladium, nickel and their combinations with other metals supported on coal, alumina, zinc oxide, and zeolites [6,9–11,14,16–21] allowing integral selectivity with respect to TL in the range of 94–99% at high NL conversions, or transforming TL to DLs under more stringent conditions. Typically, the activity of platinum-containing catalysts to produce TL is in the temperature range of 200–300 °C and pressures of 4–6 MPa. Higher temperatures cause hydrogenation of TL to DLs [10,11].

This work is devoted to selective hydrogenation of NL to TL in SC hexane as solvent over platinum NPs stabilized within hyper-cross-linked aromatic polymer (HAP) as a catalyst. For the first time, selective hydrogenation of NL to TL in SC hexane is studied.We found only one publication on the use of SC hexane for hydrogenation of aromatics, but it resultedin a ring opening and rearrangement of a carbon skeleton [22]. The aim of this work is to evaluate a potential of HAP as catalytic support for liquid-phase hydrogenation of aromatic substrates under SC conditions. The NL hydrogenation in SC hexane was used as a model reaction. We expected a higher productivity of Pt/HAP catalytic system under SC conditions due to improved masstransfer and better wettability by hexane of hydrophobic HAP, as compared to traditional hydrophilic oxides.

2. Results and Discussion

Preliminarily to NL hydrogenation, the catalyst was reduced in hydrogen flow for 3 h at 300 °C and the size of Pt NPs stabilized within HAP was characterized by Scanning Transmission Electron Microscopy (STEM) (see Figure 2). In a blank experiment under the identical reaction conditions but using the HAP without deposition of platinum, no conversion of NL was observed. This allowed us to conclude that Pt NPs are responsible for catalysis and we considered them as an active phase.

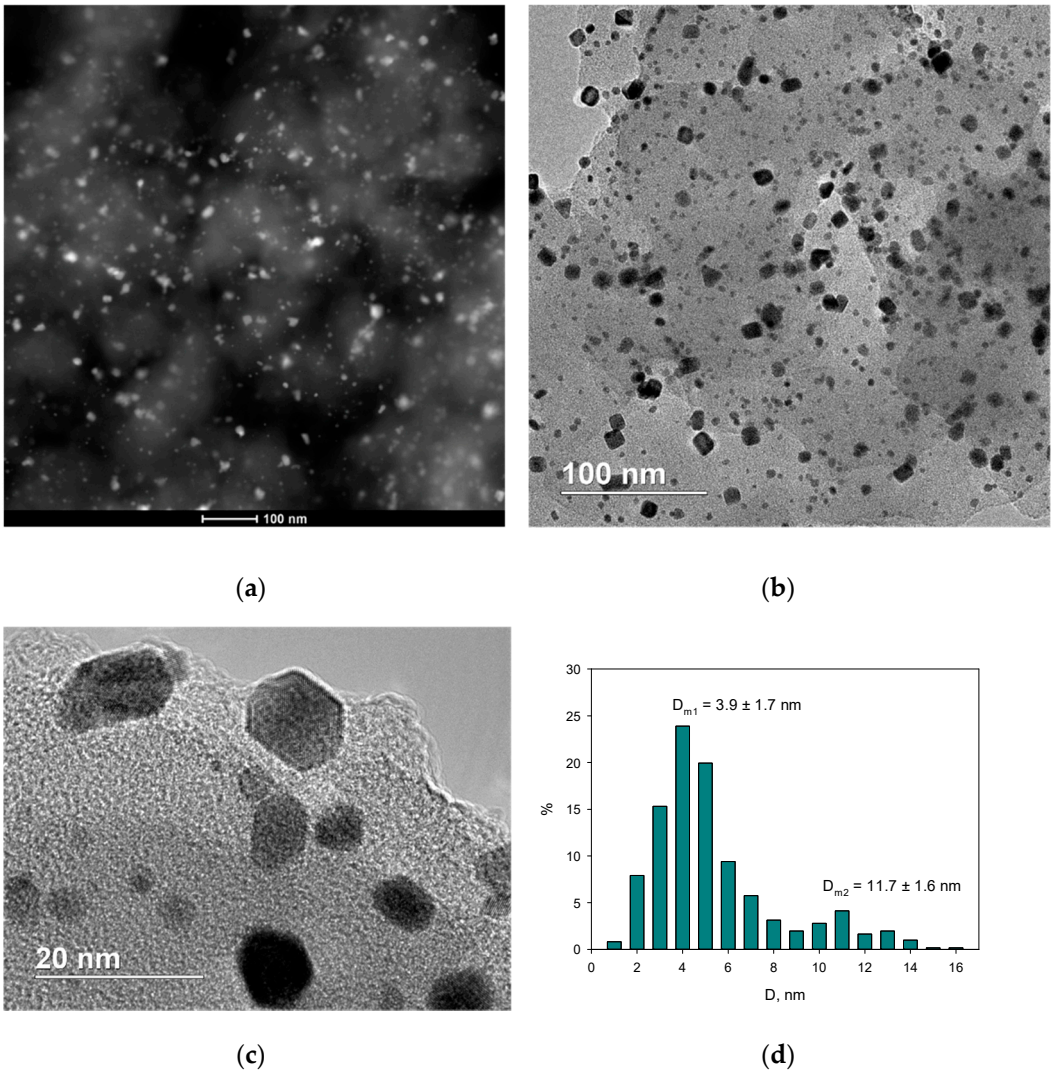

Figure 2. High-Angle Annular Dark Field Scanning Transmission Electron Microscopy (HAADF STEM) image (**a**), bright-field Transmission Electron Microscopy (TEM) images (**b**,**c**) and histogram of NPs size-distribution (**d**) of Pt/HAP (reduced for 3 h in hydrogen flow at 300 °C).

In order to optimize the yield of the target product TL, the influence of reaction temperature in the range of 240–270 °C at constant overall pressure of 5 MPa on the initial rate and selectivity was first studied. The initial reaction conditions were chosen to be higher than the critical temperature (234.5 ± 0.5 °C) and the critical pressure (3.02 ± 0.04 MPa) of pure hexane [23–28] in order to ensure the SC conditions in the reactor. It is noteworthy that the presence of NL cannot shift SC temperature and pressure to higher values since the molar ratio of hexane to NL is higher than 22, which gives an insignificant change of the critical temperature (by 0.1 °C).

As seen in Figure 3a,b, the highest initial rates of NL consumption (0.27–0.29 $mol_{NL} \cdot mol_{Pt}^{-1} \cdot s^{-1}$) and the highest selectivity to TL (about 98% at conversion close to 100%) was observed at temperatures

between 245 and 255 °C. However, at temperatures above 260 °C, the initial rate surprisingly decreases (Figure 3a). This fact can be ascribed to the change of SC fluid viscosity, which may negatively influence hydrodynamics in the reactor as well as even distribution of the catalyst inside the reactor volume—the suspended layer of catalyst granules can diminish.

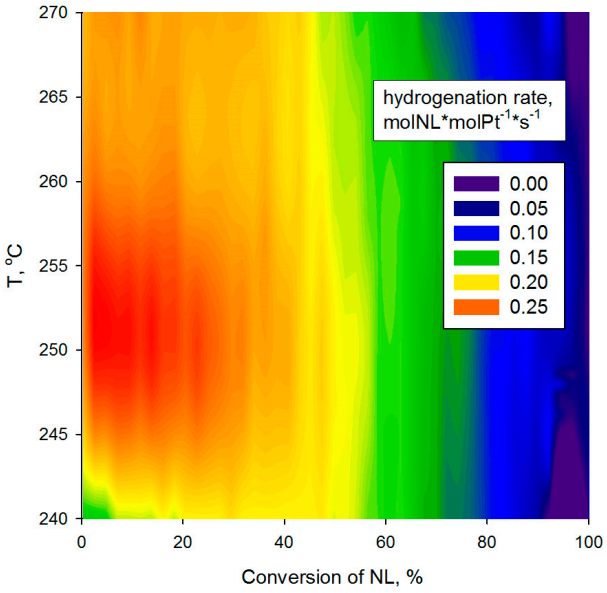

(**a**)

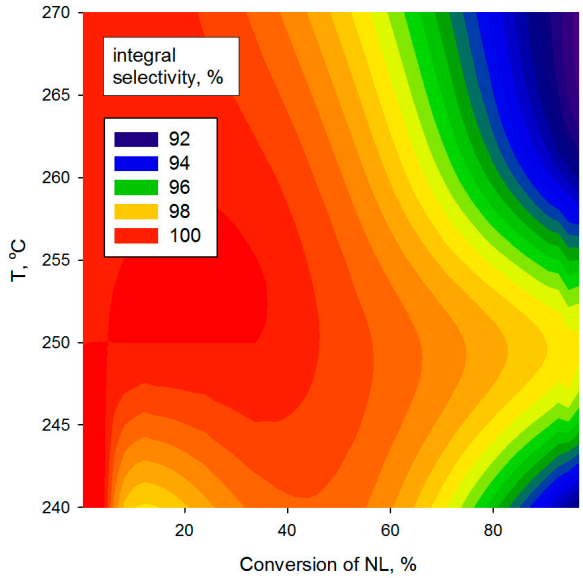

(**b**)

Figure 3. Diagrams of specific instantaneous reaction rate (**a**) and of integral selectivity with respect to TL (**b**) as a function of both NL conversion and temperature (1.5 g of NL, 0.1 g of catalyst, 40mL of hexane, 6 MPa).

The dependences of TL accumulation and the selectivity to TL on the conversion of NL are shown in Figure 3b. From the presented data, it can be seen that in the range of the substrate conversions from 0 up to 60%, NL is almost quantitatively converted to TL (Figure 3b). However, at higher conversions of NL, the concentration of TL in the reaction mixture becomes significant and the side process of

DL accumulation accelerates, which results in the decrease in the integral selectivity with respect to TL. Since temperature 250 °C allows reaching highest selectivity at high NL conversion, all further experiments were carried out at 250 °C.

After optimizing the temperature, the effect of overall pressure in the range of 5–8 MPa on the rate of NL hydrogenation and TL selectivity in the presence of Pt/HAP was studied at constant temperature of 250 °C (see Figures 4 and 5). As could be expected, the transformation rate increases with the increase in the overall pressure since partial hydrogen pressure also increases (Figure 4). The fact that the TL selectivity is close to 100% in the region of small NL conversion, allowed us to calculate the fractional reaction order with respect to H_2. It was found to be $n = 2.0$ (Figure 4a), being in agreement with the theoretical value for selective hydrogenation of NL to TL. The observed reaction order towards NL ($n = 1$) was also estimated since all the experiments were conducted under isobaric conditions.

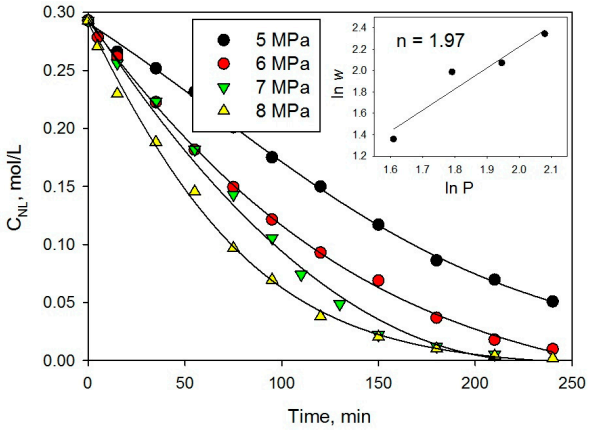

(**a**)

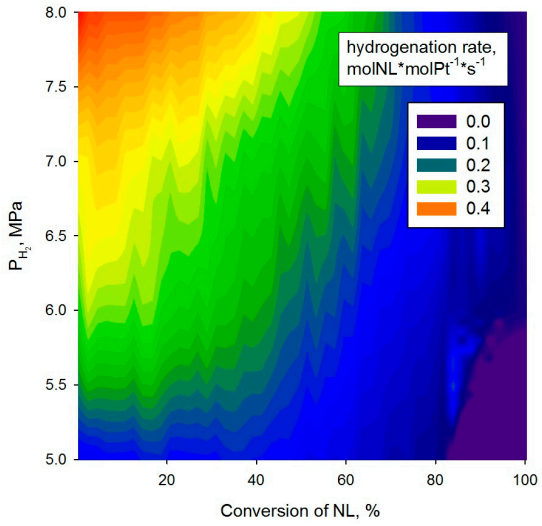

(**b**)

Figure 4. Dependence of NL consumption on time at variation of the overall pressure (**a**) and diagram of specific instantaneous reaction rate as a function of both NL conversion and pressure (**b**) (1.5 g of NL, 0.1 g of catalyst, 40 mL of hexane, 250 °C).

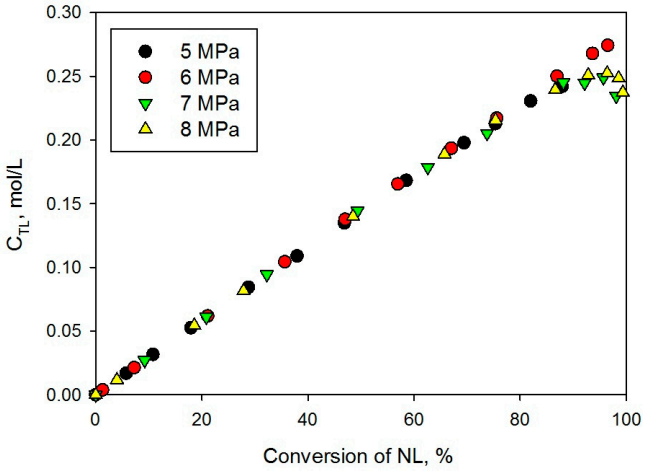

(**a**)

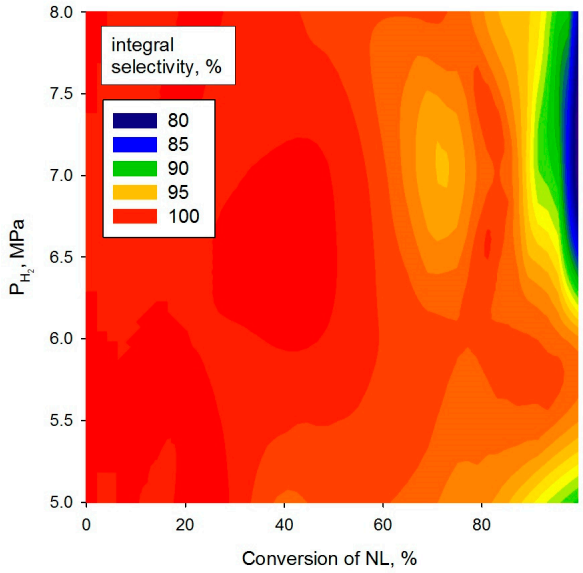

(**b**)

Figure 5. Dependence of TL accumulation on the conversion of NL at variation of the overall pressure (**a**) and diagram of integral selectivity with respect to TL as a function of both NL conversion and pressure (**b**) (1.5 g of NL, 0.1 g of catalyst, 40 mL of hexane, 250 °C).

Unfortunately, the increase in partial hydrogen pressure above 6 MPa results in decrease in TL selectivity at NL conversion > 60%. This could be explained by the higher rate of side reaction (TL to DL transformation) (Figure 5a). At the same time, the observed selectivity close to 100% during the whole range of NL conversions can be achieved at the overall pressure of about 6 MPa (Figure 5b). Therefore, 6 MPa at 250 °C was determined as the optimal condition in view highest TL yield attained in this catalytic system.

It is well known that the polymeric network may influence, to some extent, the nucleation and growth of metal NPs [29–31], which can in turn have a significant impact on catalytic activity and selectivity. Therefore, in the reaction of NL hydrogenation, a series of experiments was carried out

at chosen temperature of 250 °C and overall pressure in the reactor of 6 MPa, in which Pt-HAP was preliminarily reduced in hydrogen flow at 300 °C for 3, 12, and 24 h.

From the kinetic curves shown in Figure 6a, it is obvious that the increase in duration of the catalyst reduction from 3 h up to 12 h resulted in twofold of the rate of NL consumption (initial hydrogenation rates were 0.26 $mol_{NL} \cdot mol_{Pt}^{-1} \cdot s^{-1}$ and 0.48 $mol_{NL} \cdot mol_{Pt}^{-1} \cdot s^{-1}$, respectively). Further increase in the reduction duration up to 24 h did not lead to an increase in the observed hydrogenation rate (0.46 $mol_{NL} \cdot mol_{Pt}^{-1} \cdot s^{-1}$). At the same time, it is noteworthy that in the presence of the catalysts with a long-time preliminary reduction, at high NL conversions the increase in the rate of side products (DLs) accumulation occurs and TL concentration drops (Figure 6b). The values of the integral selectivity calculated at 70% of NL conversion of 98.4%, 96.5% and 95.6% were achieved for the samples reduced for 3 h, 12 h and 24 h, respectively, but at higher conversion (96%) the difference in selectivity was more pronounced: 97.0%, 85.0%, and 79.2%. In other words, for Pt-HAP, the increase in reduction duration contributes to disproportionate increase in hydrogenation rates of NL to TL and TL to DL.

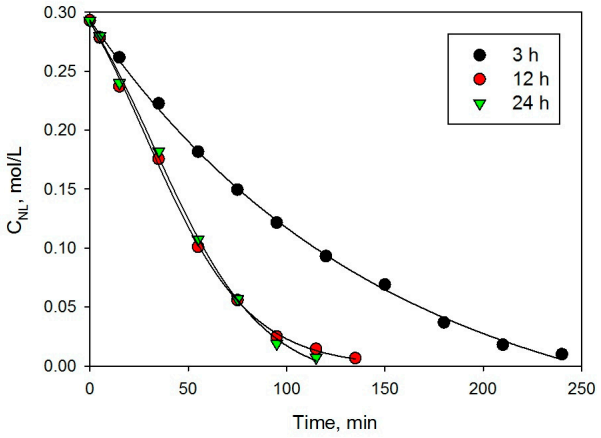

(**a**)

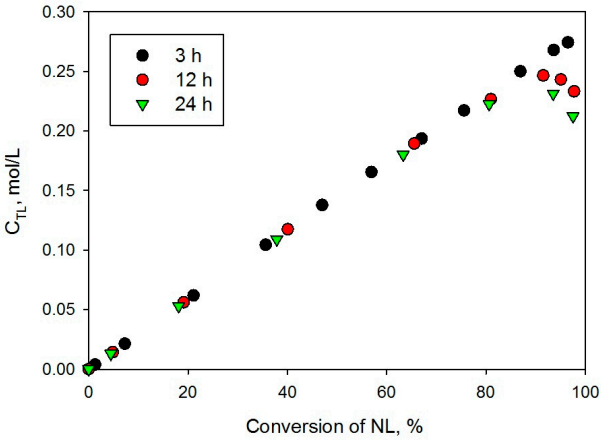

(**b**)

Figure 6. Dependence of NL consumption on time (**a**) and accumulation of TL on the NL conversion (**b**) at variation of duration of the catalyst reduction (1.5 g of NL, 0.1 g of catalyst, 40 mL of hexane, 250 °C, 6 MPa).

To find if any changes in the composition and functional groups of HAP and also the chemical state of platinum occurred during the reduction as well as during the catalytic process, Diffuse Reflectance Infrared Fourier Transform Spectroscopy (DRIFTS) and X-Ray Photoelectron Spectroscopy (XPS) studies of the catalysts were carried out.

Normalized IR-spectra of the initial and reduced catalyst are shown in Figure 7. It can be seen that, for all the samples, the spectra are in accordance with their chemical nature characterized by the following: the absorption bands at 3047 and 3018 cm^{-1} belonging to stretching vibrations of C–H bond in aromatic rings; 1610 and 1507 cm^{-1} belonging to stretching vibrations of C–C bond in aromatic rings; 2000–1650 and 815 cm^{-1} associated with the composite vibrations of *p*-substituted benzene rings. Absorption bands at 3000–2840 cm^{-1} correspond to stretching vibrations of C–H bond of the alkane part of HAP. The absorption bands in the range of 1470–700 cm^{-1} correspond to the deformation (torsion, rolling, pendulum) vibrations of CH_2 and CH_3 groups, while 1400–1000 cm^{-1} can be also attributed to stretching vibrations of C–N in tertiary amines, which are present in the chosen type of HAP [32,33]. The absorption band at about 3650 cm^{-1} refers to the vibrations of OH–groups of the polymer and water, which did not form hydrogen bonds; the bands in the region of 3500–3200 cm^{-1} belong to stretching vibrations of OH– groups that formed hydrogen bonds; 1012 cm^{-1} belong to stretching vibrations of C–O bond in alcohols; 567 cm^{-1} associated with extra plane vibrations of OH– group.

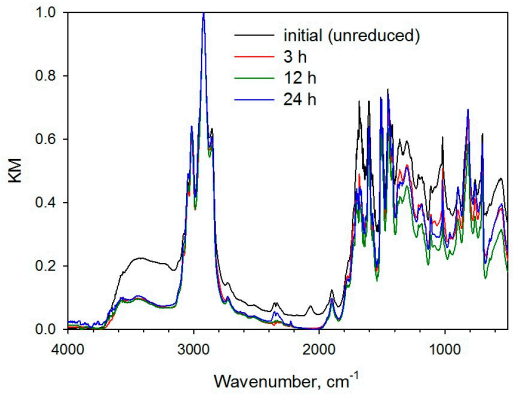

(**a**)

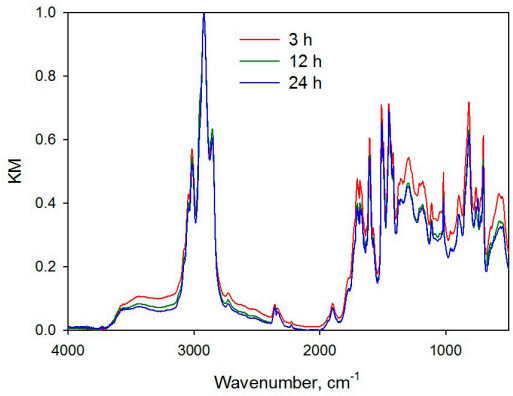

(**b**)

Figure 7. Normalized IR-spectra of Pt-HAP (unreduced (black line) and reduced for 3 h (red line), 12 h (green line) and 24 h (blue line)) (**a**) and of the three preliminarily reduced samples taken after the NL hydrogenation (**b**).

The absorption bands at 1780 and 1678 cm^{-1} in the polymer structure are the most controversial ones. In accordance with the reference data, their position corresponds to stretching vibrations of

>C=O belonging to keto- and carboxyl groups. The wide range of 1790–1650 cm^{-1} can be attributed to stretching vibrations of >C=O group in esters [32,33], in which the band at about 1760 cm^{-1} can be ascribed to stretching vibrations of >C=O in esters of phenols and aliphatic acids, while the band at about 1735 cm^{-1} refers to stretching vibrations of >C=O belonging to esters of phenols and aromatic acids. However, the results obtained by Davankov et al. for hyper-cross-linked polystyrene [34] allow us assuming that the absorption bands in the region of 1740–1600 cm^{-1}, as well as the band at 1604 cm^{-1}, can be attributed to hindered vibrations of C–C bonds and bond angles in benzene rings.

From the data presented in Figure 7a it can be concluded that the reduction of the synthesized Pt-containing HAP-based catalyst at 300 °C for 3 h results in noticeable decrease in the signal intensity in the range of 3600–3200 cm^{-1}, 1012 and 567 cm^{-1}, which is likely due to the decrease in content of OH–groups and water. The shift of the absorption band of stretching vibrations of OH-groups to 3500 cm^{-1} indicates the decrease in OH– groups involved in the formation of hydrogen bonds. In this case, the absorption band at 1678 cm^{-1} is split into two components 1678 and 1796 cm^{-1}, which can be associated with the destruction of carboxyl and ester groups [32,33] or partial destruction of stressed structures in the HAP network [34]. Further thermal treatment under hydrogen atmosphere with the duration up to 24 h does not cause significant changes in the composition of the functional groups of Pt-HAP.

FTIR spectra of the reduced catalyst samples taken after the reaction of NL hydrogenation slightly differ from each other (Figure 7b). The only difference can be pointed out is insignificant decrease in the content of oxygen-containing functional groups and tense sites of the polymer chain, as evidenced by the decrease in the intensity of absorption bands at 1678 and 1796 cm^{-1}.

XPS analysis revealed that the surface of all the samples (initial, reduced and taken after the NL hydrogenation) contains carbon, oxygen, nitrogen and platinum (Table 1).

Table 1. Elemental composition of the catalyst surface.

Element and Band	Surface Content, at.%						
	Initial (Unreduced) Catalyst	After the Reduction			After the Use in NL Hydrogenation		
		3 h	12 h	24 h	3 h	12 h	24 h
Pt 4f	1.6	1.4	1.4	1.4	1.2	1.1	1.1
Cl 2p	1.4	0.4	0.3	0.1	0.2	0.2	0.1
C 1s	83.6	91.8	92.3	92.9	91.0	90.4	90.9
O 1s	10	5.2	5.0	4.9	6.6	7.0	6.7
N 1s	3.4	1.2	1.0	0.9	1.0	1.3	1.2

The reduction of the initial catalytic system for 3 h leads to the decrease in the oxygen content on the surface in 1.9 times. Further reduction up to 12 and 24 h leads to slight decrease in the oxygen content on the surface (in 2 and 2.1 times, respectively, in comparison with the unreduced sample). This fact is in good agreement with FTIR data (see Figure 7a), which demonstrated the decrease in the intensity of absorption bands belonging to oxygen-containing groups after the first three hours of reduction.

Model deconvolution of C 1s (Figure 8a) sublevel for Pt-HAP (initial and reduced for 3 h) shows that the OH-groups associated with HAP are almost completely removed from the catalyst surface after the reduction (Figure 8b,c). The surface content of carboxyl or ester groups decreases in about 2 times, and the content of amino groups of the polymeric matrix slightly decreases, which is in good agreement with FTIR data. At the same time, removal of the significant part of the residual Cl^- (Table 1) occurs, possibly remaining after the decomposition of chloroplatinic acid from the surface.

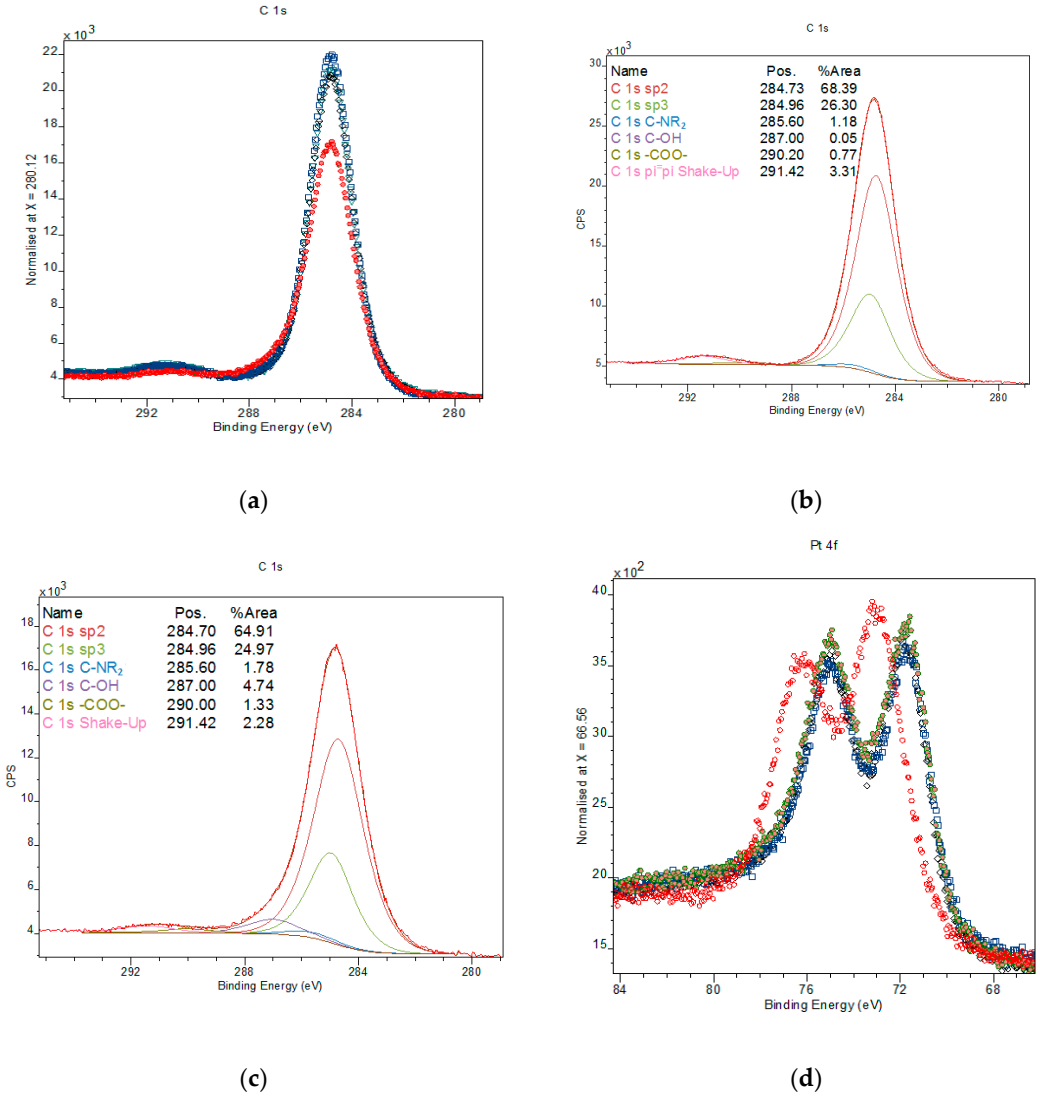

Figure 8. High-resolution spectrum of C 1s (**a**) for initial Pt-HAP (red circles) and the samples reduced for 3 h (green triangles), 12 h (blue squares) and 24 h (black rhombs) and deconvolution of C 1 s of the Pt-HAP (initial (**b**) and reduced for 3 h (**c**)) and high-resolution spectrum of Pt 4f (**d**).

The content of Pt on the catalyst surface decreases slightly after the treatment in H_2 flow for 3 h, and, after that, it remains constant for all the reduced samples, regardless the reduction duration (Table 1).

In the case of the samples taken after the use in hydrogenation of NL, slight decrease in platinum content (by 0.2–0.3 at.%) accompanied by the increase in oxygen content (by 1.5–2.0 at.%) can be found (see Table 1) in comparison with the initial preliminarily reduced samples. This fact is likely due to the adsorption of TL and oxygen of air on the surface of HAP, since all the samples were washed with hexane and dried in air after the catalytic experiments.

Analysis of high-resolution spectra of Pt 4f (see Figure 8d and Figure S1) revealed that, for the initial (unreduced) catalyst, the component $4f_{7/2}$ has binding energy of 72.9 eV, which corresponds to platinum (II) oxide [35]. For all the reduced samples, binding energy of Pt $4f_{7/2}$ is 71.4 eV, which can be ascribed to Pt(0) [35].

The stability of Pt-HAP (preliminarily reduced for 3 h in hydrogen flow) was studied in four consecutive runs. After the completion of NL hydrogenation, the catalyst was filtered under vacuum using membrane filter (0.45 μm pore size), washed with hexane and dried till constant weight at 70 °C.

It is noteworthy that the catalyst weight remained the same in each run: several (at least 3) catalyst samples were collected from previous runs and average catalyst sample was taken for further run to keep all the reaction conditions unchanged. It was found that after the first use in NL hydrogenation the reaction rate increases in about 1.2 times; after that, it stabilized, while selectivity with respect to TL remained constant (in the range of 93–94%). For comparison, Su et al. recently reported 99.75% TL selectivity achieved at 95.62% NL conversion in hexane medium using 4 wt.%NiO-20 wt.%MoO_3/Al_2O_3 catalyst at 200 °C and 6 MPa of hydrogen for 8 h in a batch mode. However, noticeable decrease in NL conversion was observed in the second reaction run that was likely due to the loss of active metals [14].

3. Materials and Methods

3.1. Materials

HAP (Macronet MN100 (Purolite Int., Wales, UK), which is hyper-cross-linked polystyrene bearing tertiary amino groups) was washed with distilled water and acetone and dried under vacuum as described elsewhere [36]. Naphthalene (NL, 99%), tetrahydrofuran (THF, ≥99.9%) and hexane (≥99%), were obtained from Sigma-Aldrich. Chloroplatinic acid hydrate (H_2PtCl_6*$6H_2O$, Pt content 38.41%) was purchased from JSC "Aurat" (Moscow, Russia). All chemicals were used as received. Distilled water was purified with an Elsi-Aqua water purification system.

3.2. Catalyst Synthesis

Pt-NPs HAP-based catalyst was synthesized via wet-impregnation according to procedure, which is described elsewhere [37]. In a typical experiment, 1 gof pretreated, dried and crushed (<63 μm) granules of HAP were impregnated with 2.8 mL of the THF solution of precursor (H_2PtCl_6*$6H_2O$) of a choosen concentration. The Pt-impregnated HAP wasdried, washed with distilled water until a neutral pH was obtained, and dried again at70 °C until the constant weight was achieved. Thus, the catalysts Pt/HAP was synthesized containing 1.0 wt.% of Pt (confirmed by the elemental analysis).

This catalyst was reduced in a hydrogen flow (100 mL/min) at 300 °C for 3 h at variation of reduction duration: 3 h, 12 h or 24 h

3.3. Catalytic Testing

Testing of Pt-HAP was carried out in a stainless steel autoclave reactor (Parr Instruments, Moline, IL, USA) having internal volume of 80 mL. In a typical experiment, 0.1 g of preliminarily reduced Pt/HAP was placed in the reactor. Then 1.5 g of NL and 40 mL of hexane were added. After that the reactor was sealed, purged with nitrogen and heated under stirring (1500 rpm) up to operating temperature at 5 MPa of N_2. After reaching working temperature, the first sample of the reaction mixture was taken. Then nitrogen was replaced with hydrogen, overall working pressure was attained (time "zero" for the reaction) and the reaction was started. Sampling of the reaction mixture was carried out via long narrow capillary (internal diameter of 0.1 mm); the volume of each sample was 200 μL.

Composition of the reaction mixture was identified via GC-MS (Shimadzu GCMS-QP2010S) equipped with a capillary column HP-1 MS (100 m × 0.25 mm i.d., 0.25 μm film thickness). Helium was used as a carrier gas at pressure of 74.8 kPa and linear velocity of 36.3 cm/s. Oven temperature was programmed: 120 °C (0 min) → 10 °C/min (160 °C) → 25 °C/min (300 °C) → 300 °C (2.4 min). Temperature of injector, interface and ion source was at 260 °C, range from 10 up to 500 m/z.

Quantitative analysis of reaction mixture was carried out via GC (Kristallux 4000 M) equipped with FID and capillary column ZB-WAX (60 m × 0.53 mm i.d., 1 μm film thickness). Temperature of detector and injector was 240 °C. Column temperature was programmed as follows: 50 °C (5 min), then heating up to 90 °C (10 °C/min) and then up to 160 °C (40 °C/min) and finally 160 °C for 5 min. Helium (30 mL/min) was used as a carrier gas. The concentrations of the reaction mixture components were calculated using absolute calibration method using chemically pure components.

The resulting "concentration vs. time" dependences were approximated by spline curves, which were used for calculation of NL conversion and specific instantaneous reaction rate.

Conversion of NL was defined as

$$X_{NL}\ (\%) = (C_{NL,0} - C_{NL}) \times C_{NL,0}{}^{-1} \times 100 \quad (1)$$

Integral selectivity with respect to TL was given as

$$S_{TL}\ (\%) = C_{TL} \times (C_{NL,0} - C_{NL})^{-1} \times 100 \quad (2)$$

Specific instantaneous reaction rate was designated as w, [$mol_{NL} \cdot mol_{Pt}{}^{-1} \cdot s^{-1}$].

$$w = dC_{NL} \times C_{Pt}{}^{-1} \times d\tau^{-1} \quad (3)$$

where C_{NL} and C_{Pt} are concentrations (mol/L) of NL and Pt, respectively, and τ is the reaction time (s).

3.4. Catalyst Characterization

Pt/HAP catalyst was characterized by liquid nitrogen physisorption, X-Ray Photoelectron Spectroscopy (XPS), Diffuse Reflectance Infrared Fourier Transform Spectroscopy (DRIFTS) and Scanning Transmission Electron Microscopy (STEM).

DRIFTS was carried out using an IRPrestige-21 FTIR spectrometer (Shimadzu, Kyoto, Japan) equipped with a DRS-8000 diffuse reflectance accessory (Shimadzu, Kyoto, Japan). The background sample was a mirror of the material of the optical system of the DRS-8000 accessory. All spectra were recorded in the 4000–500 cm^{-1} range of wavenumbers at a resolution of 4 cm^{-1}.

XPS data were obtained using Mg Kα (hν = 1253.6 eV) radiation with ES-2403 spectrometer (Institute for Analytic Instrumentation of RAS, St.Petersburg, Russia) equipped with energy analyzer PHOIBOS 100-MCD5 (SPECS, Berlin, Germany) and X-Ray source XR-50 (SPECS, Berlin, Germany). All the data were acquired at X-ray power of 250 W. Survey spectra were recorded at an energy step of 0.5 eV with an analyzer pass energy 40 eV, and high-resolution spectra were recorded at an energy step of 0.05 eV with an analyzer pass energy 7 eV. Samples were allowed to outgas for 180 min before analysis and were stable during the examination. The data analysis was performed by CasaXPS.

STEM characterization was carried out using FEI Tecnai Osiris instrument (Thermo Fisher Scientific, Waltham, MA, USA) operating at an accelerating voltage of 200 kV, equipped with high-angle annular dark field (*HAADF*) detector (Fischione, Export, PA, USA) and energy-dispersive X-ray (*EDX*) microanalysis spectrometer (EDAX, Mahwah, NJ, USA). Samples were prepared by embedding the catalyst in epoxy resin with following microtomming (*ca.* 50 nm thick) at ambient temperature. For the image processing Digital Micrograph (Gatan, Pleasanton, CA, USA) software and TIA (Thermo Fisher Scientific, Waltham, MA, USA) were used. Holey carbon/Cu grid was used as a sample support.

4. Conclusions

We have shown for the first time that NL can be hydrogenated selectively to TL in SC hexane using Pt-NPs stabilized within HAP network. HAP was shown to be relatively stable at the reaction conditions used (250 °C, 6 MPa) as well as during the activation in hydrogen flow at 300 °C. The use of supercritical hexane conjugated with such heterogeneous catalytic system is advantageous for NL selective hydrogenation to TL as hexane after depressurizing can be easily separated from the reaction products by simple cooling of the final reaction mixture. The Pt/HAP catalyst was stable in four consecutive reaction runs without loss of activity and electivity.

Supplementary Materials: The following are available online at http://www.mdpi.com/2073-4344/10/11/1362/s1, Figure S1: Deconvolution of Pt 4f for Pt-HAP: initial (**a**) and reduced for 3 h (**b**).

Author Contributions: Conceptualization, A.V.B.; methodology, A.V.B. and L.N.; software, A.V.B.; validation, L.K.-M., A.V.B. and L.N.; formal analysis, D.V.A., G.N.D.; investigation, D.V.A., G.N.D., A.L.V.; resources, L.K.-M.; data curation, A.V.B., D.V.A., G.N.D., A.L.V.; writing—original draft preparation, A.V.B.; writing—review and editing, L.K.-M. and L.N.; visualization, A.V.B., A.L.V. and L.N.; supervision, A.V.B., L.K.-M. and L.N.; project administration, L.K.-M.; funding acquisition, L.K.-M. and L.N. All authors have read and agreed to the published version of the manuscript.

Funding: The Russian Foundation for Basic Research (project 18-08-00435) supported the work concerning physicochemical studies; the Russian Science Foundation (project 20-19-00386) supported the catalysts synthesis and their testing in NL hydrogenation as well as the manuscript preparation.

Acknowledgments: The authors highly appreciate the work of Irina Yu. Tiamina on the catalysts preparation.

Conflicts of Interest: The authors declare no competing financial interest.

Abbreviations: NP: nanoparticle; HAP: hyper-cross-linked aromatic polymer; NL: naphthalene; TL: tetralin; DL: decalin.

References

1. Zhang, H.; Li, H.; Hu, Y.; Rao, K.T.V.; Xu, C.; Yang, S. Advances in production of bio-based ester fuels with heterogeneous bifunctional catalysts. *Renew. Sustain. Energy Rev.* **2019**, *114*, 109296. [CrossRef]
2. Somorjai, G.A.; Frei, H.; Park, J.Y. Advancing the frontiers in nanocatalysis, biointerfaces, and renewable energy conversion by innovations of surface techniques. *J. Am. Chem. Soc.* **2009**, *131*, 6589–6605. [CrossRef]
3. Baiker, A. Supercritical Fluids in Heterogeneous Catalysis. *Chem. Rev.* **1999**, *99*, 453–474. [CrossRef]
4. Kumar, V.; Nigam, K.D.P. Process intensification in green synthesis. *Green Process. Synth.* **2012**, *1*, 79–107. [CrossRef]
5. Hart, A.; Adam, M.; Robinson, J.P.; Rigby, S.P.; Wood, J. Hydrogenation and dehydrogenation of tetralin and naphthalene to explore heavy oil upgrading using $NiMo/Al_2O_3$ and $CoMo/Al_2O_3$ catalysts heated with steel balls via induction. *Catalysts* **2020**, *10*, 497. [CrossRef]
6. Feiner, R.; Schwaiger, N.; Pucher, H.; Ellmaier, L.; Derntl, M.; Pucher, P.; Siebenhofer, M. Chemical loop systems for biochar liquefaction: Hydrogenation of naphthalene. *RSC Adv.* **2014**, *4*, 34955–34962. [CrossRef]
7. Feiner, R.; Schwaiger, N.; Pucher, H.; Ellmaier, L.; Pucher, P.; Siebenhofer, M. Liquefaction of pyrolysis derived biochar: A new step towards biofuel from renewable resources. *RSC Adv.* **2013**, *3*, 17898–17903. [CrossRef]
8. Feiner, R.; Schwaiger, N.; Pucher, H.; Ellmaier, L.; Reiter, A.; Derntl, M.; Glatz, T.; Pucher, P.; Siebenhofer, M. Kinetics of biochar liquefaction. *BioEnergy Res.* **2014**, *7*, 1343–1350. [CrossRef]
9. Bie, S.; Jiang, H.; Wang, W.; Shu, G.; Zhang, X.; Wang, H.; Gao, S. Kinetics of naphthalene catalytic hydrogenation under high temperature and high pressure. *Petrol. Sci. Technol.* **2020**, *38*, 266–270. [CrossRef]
10. He, T.; Wang, Y.; Miao, P.; Li, J.; Wu, J.; Fang, Y. Hydrogenation of naphthalene over noble metal supported on mesoporous zeolite in the absence and presence of sulfur. *Fuel* **2013**, *106*, 365–371. [CrossRef]
11. Albonetti, S.; Baldi, G.; Barzanti, A.; Castellon, E.R.; Lopez, A.J.; Quesada, D.E.; Vaccari, A. NanosizedPd/Pt and Pd/Rh catalysts for naphthalene hydrogenation and hydrogenolysis/ring-opening. *Catal. Lett.* **2006**, *108*, 197–207. [CrossRef]
12. Luo, M.; Wang, Q.; Zhang, X.; Hu, B. The reactants' phase state: A nonnegligible factor in tetralin hydrogenation catalysts evaluation. *Int. J. Chem. Eng.* **2014**, *2014*, 405703. [CrossRef]
13. Cheng, Y.; Fan, H.; Wu, S.; Wang, Q.; Guo, J.; Gao, L.; Zong, B.; Han, B. Enhancing the selectivity of the hydrogenation of naphthalene to tetralin by high temperature water. *Green Chem.* **2009**, *11*, 1061–1065. [CrossRef]
14. Su, X.; An, P.; Gao, J.; Wang, R.; Zhang, Y.; Li, X.; Zhao, Y.; Liu, Y.; Ma, X.; Sun, M. Selective catalytic hydrogenation of naphthalene to tetralin over a $Ni\text{-}Mo/Al_2O_3$ catalyst. *Chin. J. Chem. Eng.* **2020**, *28*, 2566–2576. [CrossRef]
15. Makaryan, I.A.; Kostin, A.Y.; Sedov, I. Application of Supercritical Fluid Technologies in Chemical and Petrochemical Industries (Review). *Pet. Chem.* **2020**, *60*, 244–254. [CrossRef]
16. Liao, W.; Liu, H.-W.; Chen, H.-J.; Chang, W.-Y.; Chiu, K.-H.; Wai, C.M. Catalytic hydrogenation rate of polycyclic aromatic hydrocarbons in supercritical carbon dioxide containing polymer-stabilized palladium nanoparticles. *Chemosphere* **2011**, *82*, 573–580. [CrossRef]
17. Weitkamp, A.W. Stereochemistry and mechanism of hydrogenation of naphthalene on transition metal catalysts and conformational analysis of the products. *Adv. Catal.* **1968**, *18*, 1–110.
18. Huang, T.-C.; Kang, B.-C. Kinetic study of naphthalene hydrogenation over Pt/Al_2O_3 catalyst. *Ind. Eng. Chem. Res.* **1995**, *34*, 1140–1148. [CrossRef]

19. Huang, L.; Ge, H.; Yan, L.; Wang, G.; Qin, Z.; Wang, J. Competitive reactive adsorption desulphurization of dibenzothiophene and hydrogenation of naphthalene over Ni/ZnO. *Can. J. Chem. Eng.* **2018**, *96*, 865–872. [CrossRef]
20. Kirumakki, S.R.; Shpeizer, B.G.; Sagar, G.V.; Chary, K.V.R.; Clearfield, A. Hydrogenation of naphthalene over NiO/SiO_2-Al_2O_3 catalysts: Structure-activity correlation. *J. Catal.* **2006**, *242*, 319–331. [CrossRef]
21. Rautanen, P.A.; Lylykangas, M.S.; Aittamaa, J.R.; Krause, A.O.I. Liquid-phase hydrogenation of naphthalene and tetralin on Ni/Al_2O_3: Kinetic modeling. *Ind. Eng. Chem. Res.* **2002**, *41*, 5966–5975. [CrossRef]
22. US20110049016A1; McGrady, G.S.; Brough, S.A.; Fredericton, W. Bitumen Upgrading using Supercritical Fluids. U.S. Patent 8,691,084B2, 3 March 2011.
23. Kay, W.B. The vapor pressures and saturated liquid and vapor densities of the isomeric hexanes. *J. Am. Chem. Soc.* **1946**, *68*, 1336–1339. [CrossRef] [PubMed]
24. Ambrose, D.; Tsonopoulos, C. Vapor-liquid critical properties of elements and compounds. 2. Normal Alkenes. *J. Chem. Eng. Data* **1995**, *40*, 531–546. [CrossRef]
25. Nikitin, E.D.; Pavlov, P.A. BessonovaNCritical constants of n-alkanes with from 17 to 24 carbon atoms. *J. Chem. Thermodyn.* **1994**, *26*, 177–182. [CrossRef]
26. Nikitin, E.D.; Pavlov, P.A. SkripovPMeasurement of the critical properties of thermally unstable substances mixtures by the pulse-heating method. *J. Chem. Thermodyn.* **1993**, *25*, 869–880. [CrossRef]
27. Quadri, S.K.; Khilar, K.C.; Kudchadker, A.P.; Patni, M.J. Measurement of the critical temperatures and critical pressures of some thermally stable or mildly unstable alkanols. *J. Chem. Thermodyn.* **1991**, *23*, 67–76. [CrossRef]
28. Anselme, M.J.; Gude, M.; Teja, A.S. The critical temperatures and densities of the n-alkanes from pentane to octadecane. *Fluid Phase Equilib.* **1990**, *57*, 317–326. [CrossRef]
29. Tsvetkova, I.B.; Matveeva, V.G.; Doluda, V.Y.; Bykov, A.V.; Sidorov, A.I.; Schennikov, S.V.; Sulman, M.G.; Valetsky, P.M.; Stein, B.D.; Chen, C.-H.; et al. Pd(ii) nanoparticles in porous polystyrene: Factors influencing the nanoparticle size and catalytic properties. *J. Mater. Chem.* **2012**, *22*, 6441–6448. [CrossRef]
30. Nikoshvili, L.Z.; Nemygina, N.A.; Khudyakova, T.E.; Tiamina, I.Y.; Bykov, A.V.; Stein, B.D.; Sulman, E.M.; Kiwi-Minsker, L. Pd nanoparticles stabilized by hypercrosslinked polystyrene catalyze selective triple C-C bond hydrogenation and Suzuki cross-coupling. *J. Nanomater.* **2019**, *2019*, 6262176. [CrossRef]
31. Bronstein, L.M.; Goerigk, G.; Kostylev, M.; Pink, M.; Khotina, I.A.; Valetsky, P.M.; Matveeva, V.G.; Sulman, E.M.; Sulman, M.G.; Bykov, A.V.; et al. Structure and Catalytic Properties of Pt-Modified Hyper-Cross-Linked Polystyrene Exhibiting Hierarchical Porosity. *J. Phys. Chem. B* **2004**, *108*, 18234–18242. [CrossRef]
32. Pretsch, E.; Bühlmann, P.; Affolter, C. *Structure Determination of Organic Compounds: Tables of Spectral Data*; Springer: Berlin/Heideberg, Germany, 2000.
33. Silverstein, R.M.; Webster, F.X.; Kiemle, D.J. *Spectrometric Identification of Organic Compounds*, 7th ed.; Jonson Willey & Sons Inc.: Hoboken, NJ, USA, 2005.
34. Tsyurupa, M.P.; Blinnikova, Z.K.; Davidovich, Y.u.A.; Lyubimov, S.E.; Naumkin, A.V.; Davankov, V.A. On the nature of "functional groups" in non-functionalized hypercrosslinked polystyrenes. *React. Funct. Polym.* **2012**, *72*, 973–982. [CrossRef]
35. NIST X-Ray Photoelectron Spectroscopy Database, Version 4.1 (National Institute of Standards and Technology, Gaithersburg, 2012). Available online: http://srdata.nist.gov/xps/ (accessed on 21 November 2020).
36. Sulman, E.M.; Nikoshvili, L.Z.; Matveeva, V.G.; Tyamina, I.Y.; Sidorov, A.I.; Bykov, A.V.; Demidenko, G.N.; Stein, B.D.; Bronstein, L.M. Palladium containing catalysts based on hypercrosslinked polystyrene for selective hydrogenation of acetylene alcohols. *Top. Catal.* **2012**, *55*, 492–497. [CrossRef]
37. Doluda, V.Y.; Sulman, E.M.; Matveeva, V.G.; Sulman, M.G.; Lakina, N.V.; Sidorov, A.I.; Valetsky, P.M.; Bronstein, L.M. Kinetics of phenol oxidation over hypercrosslinked polystyrene impregnated with Pt nanoparticles. *Chem. Eng. J.* **2007**, *134*, 256–261. [CrossRef]